Supramolecular Helical Miktoarm Star Polymers

Ru Deng, Chengyuan Wang, and Marcus Weck*

Department of Chemistry and Molecular Design Institute, New York University, New York, NY 10003, United States

ABSTRACT: We report a hydrogen-bonded supramolecular miktoarm star polymer containing three distinct helical arms. Our design involves two helical poly(methacrylamide) (PMAc) arms connected by a barbituric acid (Ba) at the center, prepared through the reversible addition-fragmentation chain-transfer (RAFT) polymerization with a bifunctional agent. Together with a telechelic helical poly(isocyanide) (PIC) end-functionalized with a Hamilton Wedge (HW) that is complimentary to Ba, the two components assemble into an AB_2-type star copolymer. The assembly is driven by the hydrogen bonding between HW and Ba which is quantified by ^{1}H NMR titration and isothermal titration calorimetry (ITC). Gel-permeation chromatography (GPC) provides evidence for the formation of the desired miktoarm star architecture. This strategy of site-specific functionalization on helical polymers provides a modular approach to prepare non-linear supramolecular ensembles with topological diverse building blocks.

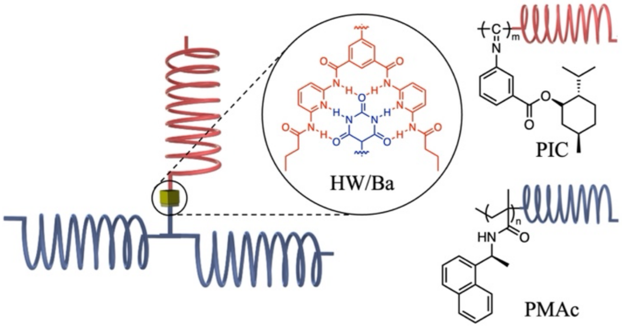

Nature utilizes noncovalent interactions to drive the arrangements of secondary structures, resulting in spatially defined protein architectures with diverse biological activities.[1] Inspired by these folding processes, the supramolecular assembly of topologically-diverse polymers has created well-defined polymeric materials.[2–5] With helical, sheet, and random-coil mimicking polymers that are functionalized with molecular recognition units (MRUs), the Weck group has reported a library of main-chain supramolecular block copolymers assembled through hydrogen bonding, metal coordination, and quadrupole interactions.[6–10] We have shown that a supramolecular block copolymer approach is an efficient route to build higher-ordered and well-characterized materials from the bottom up.

The supramolecular assemblies of secondary structure-containing building blocks into three-dimensional polymer architectures display intriguing properties that are unseen in their linear counterparts.[11] For example, a β-sheet-mimicking structure with up to five poly(*p*-phenylene vinylene) turns displays a higher degree of order with increasing number of folds.[12] We reported a supramolecular polymer brush featuring a helical backbone and coil-like poly(styrene) pendant chains connected through metal coordination, and the metallosupramolecular ensemble displayed dynamic ordering and phase segregation.[13]

Star polymers represent one of the simplest 3D-deviations from linear polymers featuring linear "arms" radiating from central branching "cores". If the arms have different chemical compositions or functionalities, the polymer is referred to as a miktoarm star.[14] The compact core-shell periphery structures of star polymers lead to unique material properties, such as altered morphologies, lower viscosities, and low melt temperatures.[14] The incorporation of secondary structure-containing building blocks into the star polymer design, especially optically-active helical polymers, increases conformational asymmetry and results in distinctive material properties and applications.[15,16] For example, a class of core-crosslinked star polymers with rigid helical arms provides confined chiral environments which allow for chiral recognition of enantiomers.[17,18] Additionally, star polymers containing one or more helical arms can lead to nanofiber aggregations and twisted ribbon nanostructures.[19–21]

Constructing complex polymer architectures with noncovalent interactions has received increasing attention in the past few decades because of the degree of flexibility and dynamics that are unachievable with covalent chemistries.[22–24] recognition pairs as block conjunctions in the star polymer design allows for modular design of individual arms, facile preparation of miktoarm star structures, and controlled responsiveness to external stimuli.[25,26] To date, the self-assemblies of supramolecular star polymers have been

Scheme 1. Synthetic route towards the bifunctional CTA containing barbituric acid (Ba-diCTA) and the preparation of helical Ba-diPMAc through RAFT polymerization.

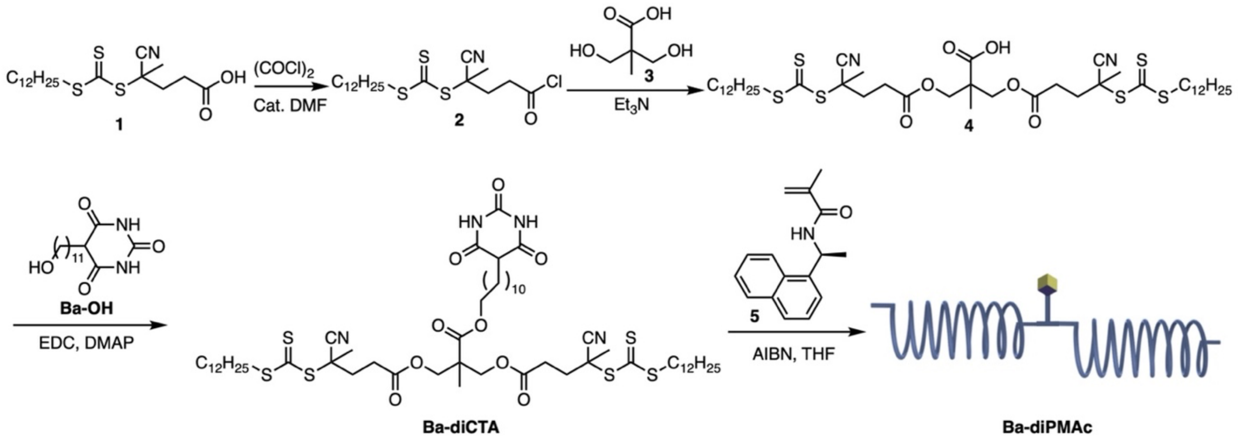

realized through hydrogen bonding,[27] metal coordination,[26] and host-guest interactions.[28] Stimuli-responsive star copolymers have been recognized as candidates for the development of smart drug-delivery vehicles.[29,30]

Supramolecularly assembled miktoarm stars featuring arms with higher-order structures have not been reported. Herein we close this gap by describing supramolecular miktoarm star polymers with three distinct helical arms. The AB$_2$-type miktoarm star contains two helical poly(methacrylamide) (PMAc) arms as well as a helical poly(isocyanide) (PIC) arm connected through the directed hydrogen bonding between a Hamilton Wedge (HW) and a barbituric acid (Ba). The sextuply hydrogen-bonded HW/Ba pair provides strong and directional interaction for supramolecular block copolymer assemblies.[31] The hydrogen bonding is characterized by ^{1}H NMR spectroscopy and isothermal titration calorimetry (ITC). The helicity of the arms is confirmed by circular dichroism (CD) spectroscopy and the successful preparation of the supramolecular star copolymer is proven by gel-permeation chromatography (GPC). The results display the potential to incorporate persistent helical structures in the fabrication of well-defined 3D supramolecular polymers.

Our polymer block design involves a telechelic, HW-functionalized helical PIC (**HW-PIC**) and a two-armed helical PMAc segmented by a barbituric acid at the center (**Ba-diPMAc**). End-functionalized, one-handed preferred helical PICs have been prepared in the literature via metal-catalyzed isocyanide polymerizations.[32–34] Compared to the well-documented strategies to install functional groups at polymer chain-ends and monomers, the site-specific functional group installation at the center of a polymer chain is less straightforward.[35] We tackle this challenge by using a bifunctional chain transfer agent (CTA) equipped with Ba (**Ba-diCTA**). Scheme 1 depicts the synthetic route. The trithiocarbonate CTA (**1**) is treated with oxalyl chloride to convert the carboxylic acid into the corresponding acid chloride (**2**), followed by the *in-situ* esterification with dimethylolpropionic acid (**3**) to afford the bifunctional CTA (**4**).[36] The hydroxyl-terminated barbituric acid (**Ba-OH**) is then installed to obtain the final **Ba-diCTA**. The successful synthesis of **Ba-diCTA** is confirmed by observing the Ba imide proton signal at δ 7.8 ppm in the ^{1}H NMR spectrum, the thiocarbonyl carbon signals at δ220 ppm in the ^{13}C NMR spectrum, and the molecular ion peak in the high-resolution mass spectroscopy (Fig. S1 and S2, Supporting Information).

The Ba-containing bifunctional agent is then used to mediate the reversible addition-fragmentation chain-transfer (RAFT) polymerization of the naphthalene-containing methacrylamide monomer (**5**), resulting in the two-armed helical **Ba-diPMAc** with a Ba group at the center. GPC measurements display a monomodal peak that corresponds to $M_{n\,GPC}$= 6,000 g/mol and a dispersity (M_w/M_n) of 1.46. Fig. 1 shows the ^{1}H NMR spectrum of **Ba-diPMAc**, where the broad peak at δ5.3-6.3 ppm represents the two protons of the amide and ethyl groups on the monomers (a, b). The broad peak at δ3.4-4.2 ppm can be assigned to the signals of six ester protons (c,e), the four protons of -S-C$\boldsymbol{H_2}$-C$_{11}$H$_{23}$ (d), and the one 1,3-dicarbonyl proton (f) on the bifunctional CTA.

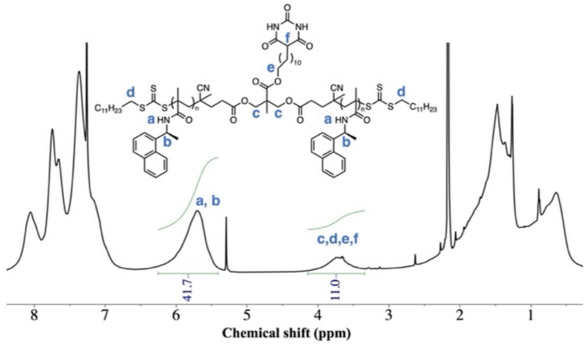

Figure 1. ^{1}H NMR spectrum of **Ba-diPMAc** ($CDCl_3$, 600 MHz) with peaks assigned to the monomers and CTA end-groups.

These CTA proton signals have been used in the end-group analysis for the trithiolcabonate CTA-generated polymers.[36,37] The area ratio of the two broad peaks suggests that the polymer has a degree of polymerization (DP) of 21 and $M_{n\,NMR}$ = 6,200 g/mol. The proximity of the results from GPC measurements and NMR end-group analysis confirms that **Ba-diPMAc** has been successfully prepared with controlled molecular weights.

The functional group analysis of **Ba-diPMAc** is carried out with MALDI-ToF mass spectroscopy. Fig. 2 displays periodic molecular ion peaks with a series of major peaks separated by 239 amu which corresponds to the molecular weight of the methacrylamide monomer (239.32 amu). The inset of Fig. 2 shows a detailed peak assignment: the molecular weights of the two peaks found match well with the corresponding polymers with 10 and 11 repeating units, respectively (n=10, found m/z = 3600.458, expected mass $[M + Na]^+$ = 3600.75). Along with the major peaks are a series of peaks with lower intensities that correspond to polymer fragmentation of the labile thioester bonds.[38] The mass distribution observed in MALDI-ToF MS does not reflect the molecular weight of the polymer because high molecular weight species cannot be analyzed by MALDI-ToF MS, as reported in the literature.[6] Therefore, the M_n value obtained from NMR end-group analysis is used to represent the molecular weight of **Ba-diPMAc**.

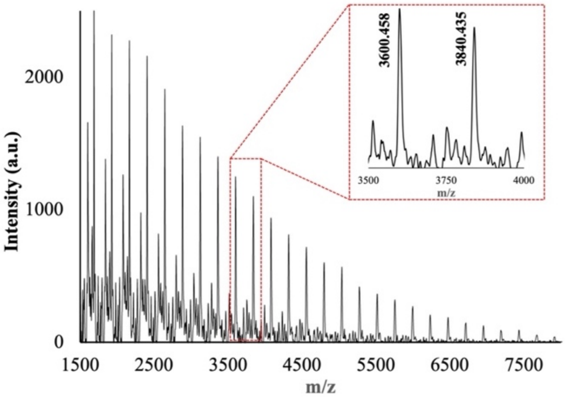

Figure 2. MALDI-ToF MS spectrum of **Ba-diPMAc**. The inset shows a partial spectrum with *m/z* values that correlate well with expected values from Ba-containing polymer species.

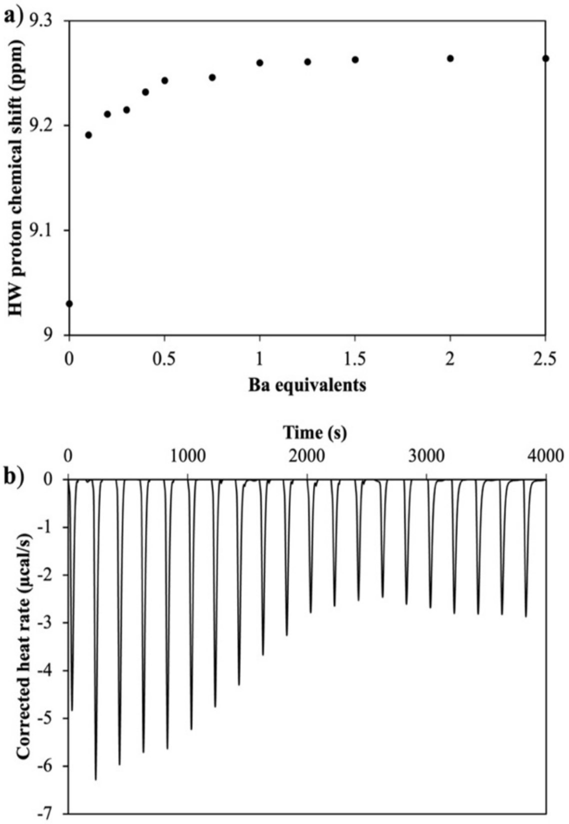

Figure 3. Titration studies to monitor the HW/Ba supramolecular interaction. (a) Representative ^{1}H NMR titration experiment ($CDCl_3$, 600 MHz, 25 °C) showing the change of HW amide proton signal as a function of Ba equivalents. (b) ITC binding isotherm between **Ba-diPMAc** and **HW-PIC**, recorded in $CHCl_3$ at 25 °C.

The miktoarm star polymer assembly through the HW/Ba recognition pair is carried out by mixing **Ba-diPMAc** and **HW-PIC** in a 1:1 ratio in chloroform. **HW-PIC** with comparable DP is prepared according to published protocols using a HW-functionalized palladium initiator.[6] The hydrogen bonding is monitored by ^{1}H NMR spectroscopy by titrating **Ba-diPMAc** into the **HW-PIC** solution in $CDCl_3$ from 0.1 to 2.5 molar equivalents. A shift of the HW amide proton signal from δ 9.03 to 9.27 ppm is observed (Fig. 3a). With increasing amount of Ba, the Ba imide proton can be resolved and its shift from δ 13.25 to 13.45 ppm is captured (Fig. S9). An average association constant ($K_{a\,NMR}$) of (1.77 ±

18%) × 10^4 M^{-1} in deuterated chloroform at 25 °C is calculated from the ^1H NMR titration experiments according to published methods.[39] This value correlates well with the association constants obtained from other HW/Ba assembled supramolecular block copolymer systems.[40]

The hydrogen bonding between HW and Ba is further characterized by ITC. **Ba-diPMAc** is titrated into **HW-PIC** over 20 injections in chloroform at 25 °C. A representative binding isotherm is shown in Fig. 3b where a subtle change in heat is captured. The average $K_{a\ ITC}$ from multiple measurements is (1.56 ± 20%) × 10^4 M^{-1}, which is comparable to the NMR titration results. In diblock copolymer systems that are connected by hydrogen bonding, increasing degree of dissociation can be observed with increasing molecular weight of the associated blocks.[6,41] Higher translational and rotational entropy values of the released blocks with higher molecular weights lead to higher dissociation values for the assembled structures.[42] In the current miktoarm system, the mass effects are offset by the use of polymer chains with lower DPs, resulting in high association constants that are comparable to the published values in the linear block copolymers.[43] Therefore, the titration studies validate the supramolecular miktoarm star polymer formation through the hydrogen bonding interaction between the HW and Ba-containing polymers.

The star polymer formation is further characterized by tracking the molecular weight change using GPC. The HW/Ba supramolecular assembly is conducted by mixing 0.02 mM stock solutions of **HW-PIC** and **Ba-PMAc** in $CHCl_3$, followed by GPC measurement with THF as the mobile phase. The GPC trace shows two peaks at 12.7 min and 15.4 min (Fig. 4). The peak at 15.4 minutes corresponds to the homoblock polymers. The peak at 12.7 minutes can be attributed to the miktoarm star polymer. The assembled block copolymer possesses higher molecular weight compared to the individual building blocks, and the rigid helical arms contribute to an extended rod-like star structure, resulting in an increased radius of gyration.[15]

The observed peak at 15.4 minutes in the miktoarm polymer sample in the GPC indicates the presence of unassembled building blocks, which we rationalize to be the result of the dynamic nature of the hydrogen bonding. In highly diluted samples, the assembled miktoarm polymers and the unassembled homoblocks are in an equilibrium. With the initial concentration for **HW-PIC** and **Ba-diPMAc** being 0.1 mM, the final product is calculated to be a mixture of 0.046 mM of miktoarm polymer and 0.054 mM of **HW-PIC** and **Ba-diPMAc** (see SI for calculation details). The peaks with comparable intensities match well with these theoretical calculations. Furthermore, the choice of solvent is an important parameter affecting hydrogen bonded polymer formation.[44] THF, a hydrogen bond acceptor, can be in competition with the HW/Ba interaction and limits the miktoarm assembly. The presented result here marks one of the few examples of visualizing supramolecular block copolymer formation via GPC measurements.

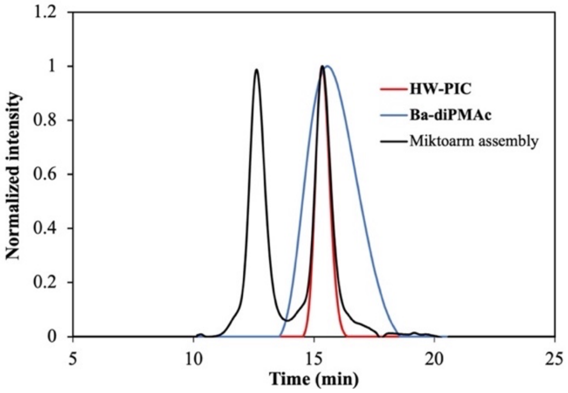

Figure 4. Normalized GPC traces of (red) **HW-PIC**, (blue) **Ba-diPMAc**, and (black) miktoarm assembly recorded in THF. The peak at 12.7 min is indicative of the miktoarm star polymer formation.

The optical activities of the helical building blocks are evaluated by CD spectroscopy in dichloroethane (DCE) at 25 °C. **HW-PIC** shows signature Cotton effects at 360 nm and 250 nm correlating to the imino and aryl chromophores in the polymer backbone, respectively (Fig 5, red).[45,46] The pattern is indicative of a predominantly left-hand preferred helix adopted by the PIC polymer backbone. The blue trace in Fig. 5 is the CD pattern of **Ba-diPMAc** under the same concentration which displays Cotton effect signals at 280 and 230 nm, indicative of a left-handed preferred PMAc helical structure.[47] The lower intensity compared to the **HW-PIC** trace can be attributed to the lower degree of polymerization of the single PMAc arm, and the intrinsically low CD intensities of the PMAc helical backbones, as observed in similar systems.[6,8,48] The miktoarm assembly is obtained from the mixture of the two helical components in 1:1 molar ratio in DCE and measured after allowing to equilibrate by stirring for ten minutes. The resulting signal (Fig. 5, black) is the sum

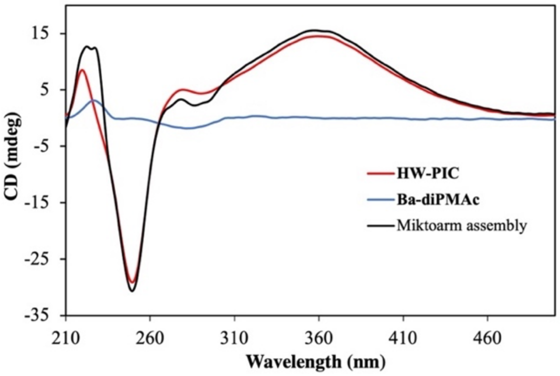

Figure 5. CD spectra of (red) **HW-PIC**, (blue) **Ba-diPMAc** and (black) miktoarm assembly recorded at 25 °C in DCE (10 μM). The miktoarm pattern reflects contributions from both PIC and PMAc helices.

of contributions from the two individual blocks: the band at 280-290 nm is impacted by the negative Cotton effect peak of **Ba-diPMAc**, while two peaks can be resolved at 220-230 nm representing the contributions from both **HW-PIC** and **Ba-diPMAc** blocks. The CD measurements therefore confirm that the one-hand preferred helical structures of both helical species are maintained in the miktoarm assembly.

In summary, we describe the synthesis of a two-armed PMAc helical polymer with Ba functionalization at the center, and the use of this building block in the supramolecular assembly of helical miktoarm star polymers. Our design utilizes the core-first approach to obtain a two-arm PMAc polymer center-functionalized with Ba, followed by the supramolecular grafting-onto approach to install the telechelic PIC helical polymer resulting in an AB_2 type miktoarm star connected by HW/Ba hydrogen bonding. Titration studies demonstrate strong hydrogen bonding and GPC measurements provide evidence of the formation of a star architecture. The helical arms maintain their distinctive one-handedness, as evidenced by CD spectroscopy. The miktoarm star assembly presented here is an important extension to the spatially defined assembly of secondary structure containing elements, which may lead to more complex polymeric ensembles.

Acknowledgement

The authors acknowledge financial support from the National Science Foundation under award number CHE-1902917. We thank Veronica Grebe for writing the MATLAB code to process the CD and GPC data.

References

(1) Anfinsen, C. B. Principles That Govern the Folding of Protein Chains. *Science* **1973**, *181*, 223–230. https://doi.org/10.1126/science.181.4096.223.

(2) Milton, M.; Deng, R.; Mann, A.; Wang, C.; Tang, D.; Weck, M. Secondary Structure in Nonpeptidic Supramolecular Block Copolymers. *Acc. Chem. Res.* **2021**, *54*, 2397–2408. https://doi.org/10.1021/acs.accounts.1c00028.

(3) Frisch, H.; Tuten, B. T.; Barner-Kowollik, C. Macromolecular Superstructures: A Future Beyond Single Chain Nanoparticles. *Isr. J. Chem.* **2020**, *60*, 86–99. https://doi.org/10.1002/ijch.201900145.

(4) Huurne, G. M. ter; Palmans, A. R. A.; Meijer, E. W. Supramolecular Single-Chain Polymeric Nanoparticles. *CCS Chem.* **2019**, *1*, 64–82. https://doi.org/10.31635/ccschem.019.20180036.

(5) Hanlon, A. M.; Lyon, C. K.; Berda, E. B. What Is Next in Single-Chain Nanoparticles? *Macromolecules* **2016**, *49*, 2–14. https://doi.org/10.1021/acs.macromol.5b01456.

(6) Croom, A.; Manning, K. B.; Weck, M. Supramolecular Helix–Helix Block Copolymers. *Macromolecules* **2016**, *49*, 7117–7128. https://doi.org/10.1021/acs.macromol.6b01410.

(7) Elacqua, E.; Croom, A.; Manning, K. B.; Pomarico, S. K.; Lye, D.; Young, L.; Weck, M. Supramolecular Diblock Copolymers Featuring Well-Defined Telechelic Building Blocks. *Angew. Chem. Int. Ed.* **2016**, *55*, 15873–15878. https://doi.org/10.1002/anie.201609103.

(8) Elacqua, E.; Manning, K. B.; Lye, D. S.; Pomarico, S. K.; Morgia, F.; Weck, M. Supramolecular Multiblock Copolymers Featuring Complex Secondary Structures. *J. Am. Chem. Soc.* **2017**, *139*, 12240–12250. https://doi.org/10.1021/jacs.7b06201.

(9) Deng, R.; Milton, M.; Pomarico, S. K.; Weck, M. Synthesis of a Heterotelechelic Helical Poly(Methacrylamide) and Its Incorporation into a Supramolecular Triblock Copolymer. *Polym. Chem.* **2019**, *10*, 5087–5093. https://doi.org/10.1039/C9PY01047E.

(10) Wang, C.; Weck, M. Intramolecular Folding of Coil-Helix Block Copolymers Induced by Quadrupole Interactions. *Macromol. Rapid Commun.* **2021**, *42* , 2100368. https://doi.org/10.1002/marc.202100368.

(11) Lutz, J.-F.; Lehn, J.-M.; Meijer, E. W.; Matyjaszewski, K. From Precision Polymers to Complex Materials and Systems. *Nat. Rev. Mater.* **2016**, *1*, 16024. https://doi.org/10.1038/natrevmats.2016.24.

(12) Elacqua, E.; Geberth, G. T.; Vanden Bout, D. A.; Weck, M. Synthesis and Folding Behaviour of Poly(p-Phenylene Vinylene)-Based β-Sheet Polychromophores. *Chem. Sci.* **2019**, *10*, 2144–2152. https://doi.org/10.1039/c8sc05111a.

(13) Deng, R.; Wang, C.; Milton, M.; Tang, D.; Hollingsworth, A. D.; Weck, M. Side-Chain Functionalized Supramolecular Helical Brush Copolymers. *Polym. Chem.* **2021**, *12*, 4916–4923. https://doi.org/10.1039/D1PY00373A.

(14) Ren, J. M.; McKenzie, T. G.; Fu, Q.; Wong, E. H. H.; Xu, J.; An, Z.; Shanmugam, S.; Davis, T. P.; Boyer, C.; Qiao, G. G. Star Polymers. *Chem. Rev.* **2016**, *116*, 6743–6836. https://doi.org/10.1021/acs.chemrev.6b00008.

(15) Hasegawa, H.; Nagata, Y.; Terao, K.; Suginome, M. Synthesis and Solution Properties of a Rigid Helical Star Polymer: Three-Arm Star Poly(Quinoxaline-2,3-Diyl). *Macromolecules* **2017**, *50*, 7491–7497. https://doi.org/10.1021/acs.macromol.7b01797.

(16) Qiu, L. Y.; Bae, Y. H. Polymer Architecture and Drug Delivery. *Pharm. Res.* **2006**, *23*, 1–30. https://doi.org/10.1007/s11095-005-9046-2.

(17) Liu, N.; Ma, C.-H.; Sun, R.-W.; Huang, J.; Li, C.; Wu, Z.-Q. Facile Synthesis and Chiral Recognition of Block and Star Copolymers Containing Stereoregular Helical Poly(Phenyl Isocyanide) and Polyethylene Glycol Blocks. *Polym. Chem.* **2017**, *8*, 2152–2163. https://doi.org/10.1039/C7PY00028F.

(18) Miyabe, T.; Iida, H.; Banno, M.; Yamaguchi, T.; Yashima, E. Synthesis and Visualization of a Core Cross-Linked Star Polymer Carrying Optically Active Rigid-Rod Helical Polyisocyanide Arms and Its Chiral Recognition Ability.

Macromolecules **2011**, *44*, 8687–8692. https://doi.org/10.1021/ma201998z.

(19) Siriwardane, D. A.; Kulikov, O.; Reuther, J. F.; Novak, B. M. Rigid, Helical Arm Stars through Living Nickel Polymerization of Carbodiimides. *Macromolecules* **2017**, *50*, 832–840. https://doi.org/10.1021/acs.macromol.6b02456.

(20) Junnila, S.; Houbenov, N.; Karatzas, A.; Hadjichristidis, N.; Hirao, A.; Iatrou, H.; Ikkala, O. Side-Chain-Controlled Self-Assembly of Polystyrene–Polypeptide Miktoarm Star Copolymers. *Macromolecules* **2012**, *45*, 2850–2856. https://doi.org/10.1021/ma202747h.

(21) Lin, Y.-A.; Ou, Y.-C.; Cheetham, A. G.; Cui, H. Supramolecular Polymers Formed by ABC Miktoarm Star Peptides. *ACS Macro Lett.* **2013**, *2*, 1088–1094. https://doi.org/10.1021/mz400535g.

(22) Schmidt, H.; Würthner, F. A Periodic System of Supramolecular Elements. *Angew. Chem. Int. Ed.* **2020**, *59*, 8766–8775. https://doi.org/10.1002/anie.201915643.

(23) Wang, L.; Cheng, L.; Li, G.; Liu, K.; Zhang, Z.; Li, P.; Dong, S.; Yu, W.; Huang, F.; Yan, X. A Self-Cross-Linking Supramolecular Polymer Network Enabled by Crown-Ether-Based Molecular Recognition. *J. Am. Chem. Soc.* **2020**, *142*, 2051–2058. https://doi.org/10.1021/jacs.9b12164.

(24) Fox, J. D.; Rowan, S. J. Supramolecular Polymerizations and Main-Chain Supramolecular Polymers. *Macromolecules* **2009**, *42*, 6823–6835. https://doi.org/10.1021/ma901144t.

(25) Schmidt, B. V. K. J.; Kugele, D.; von Irmer, J.; Steinkoenig, J.; Mutlu, H.; Rüttiger, C.; Hawker, C. J.; Gallei, M.; Barner-Kowollik, C. Dual-Gated Supramolecular Star Polymers in Aqueous Solution. *Macromolecules* **2017**, *50*, 2375–2386. https://doi.org/10.1021/acs.macromol.7b00165.

(26) Hou, Z.; Dehaen, W.; Lyskawa, J.; Woisel, P.; Hoogenboom, R. A Supramolecular Miktoarm Star Polymer Based on Porphyrin Metal Complexation in Water. *Chem. Commun.* **2017**, *53*, 8423–8426. https://doi.org/10.1039/C7CC03128A.

(27) Todd, E. M.; Zimmerman, S. C. Supramolecular Star Polymers. Increased Molecular Weight with Decreased Polydispersity through Self-Assembly. *J. Am. Chem. Soc.* **2007**, *129*, 14534–14535. https://doi.org/10.1021/ja075453j.

(28) Yebeutchou, R. M.; Tancini, F.; Demitri, N.; Geremia, S.; Mendichi, R.; Dalcanale, E. Host–Guest Driven Self-Assembly of Linear and Star Supramolecular Polymers. *Angew. Chem. Int. Ed.* **2008**, *47*, 4504–4508. https://doi.org/10.1002/anie.200801002.

(29) Fan, X.; Cheng, H.; Wang, X.; Ye, E.; Loh, X. J.; Wu, Y.-L.; Li, Z. Thermoresponsive Supramolecular Chemotherapy by "V"-Shaped Armed β-Cyclodextrin Star Polymer to Overcome Drug Resistance. *Adv. Healthc. Mater.* **2018**, *7*, 1701143. https://doi.org/10.1002/adhm.201701143.

(30) Tucker, B. S.; Getchell, S. G.; Hill, M. R.; Sumerlin, B. S. Facile Synthesis of Drug-Conjugated PHPMA Core-Crosslinked Star Polymers. *Polym. Chem.* **2015**, *6*, 4258–4263. https://doi.org/10.1039/C5PY00497G.

(31) Yang, S. K.; Zimmerman, S. C. Hydrogen Bonding Modules for Use in Supramolecular Polymers. *Isr. J. Chem.* **2013**, *53*, 511–520. https://doi.org/10.1002/ijch.201300045.

(32) Xue, Y.-X.; Zhu, Y.-Y.; Gao, L.-M.; He, X.-Y.; Liu, N.; Zhang, W.-Y.; Yin, J.; Ding, Y.; Zhou, H.; Wu, Z.-Q. Air-Stable (Phenylbuta-1,3-Diynyl)Palladium(II) Complexes: Highly Active Initiators for Living Polymerization of Isocyanides. *J. Am. Chem. Soc.* **2014**, *136*, 4706–4713. https://doi.org/10.1021/ja5004747.

(33) Zhou, L.; Xu, X.; Jiang, Z.; Xu, L.; Chu, B.; Liu, N.; Wu, Z. Selective Synthesis of Single-Handed Helical Polymers from Achiral Monomer and a Mechanism Study on Helix-Sense-Selective Polymerization. *Angew. Chem. Int. Ed.* **2021**, *60*, 806–812. https://doi.org/10.1002/anie.202011661.

(34) Liu, N.; Zhou, L.; Wu, Z.-Q. Alkyne-Palladium(II)-Catalyzed Living Polymerization of Isocyanides: An Exploration of Diverse Structures and Functions. *Acc. Chem. Res.* **2021**, *54*, 3953–3967. https://doi.org/10.1021/acs.accounts.1c00489.

(35) Matyjaszewski, K.; Tsarevsky, N. V. Nanostructured Functional Materials Prepared by Atom Transfer Radical Polymerization. *Nat. Chem.* **2009**, *1*, 276–288. https://doi.org/10.1038/nchem.257.

(36) Gao, C.; Li, S.; Li, Q.; Shi, P.; Shah, S. A.; Zhang, W. Dispersion RAFT Polymerization: Comparison between the Monofunctional and Bifunctional Macromolecular RAFT Agents. *Polym. Chem.* **2014**, *5*, 6957–6966. https://doi.org/10.1039/C4PY01069H.

(37) Bivigou-Koumba, A. M.; Kristen, J.; Laschewsky, A.; Müller-Buschbaum, P.; Papadakis, C. M. Synthesis of Symmetrical Triblock Copolymers of Styrene and *N*-Isopropylacrylamide Using Bifunctional Bis(Trithiocarbonate)s as RAFT Agents. *Macromol. Chem. Phys.* **2009**, *210*, 565–578. https://doi.org/10.1002/macp.200800575.

(38) Chen, S.; Ströhl, D.; Binder, W. H. Orthogonal Modification of Polymers via Thio–Bromo "Click" Reaction and Supramolecular Chemistry: An Easy Method Toward Head-to-Tail Self-Assembled Supramolecular Polymers. *ACS Macro Lett.* **2015**, *4*, 48–52. https://doi.org/10.1021/mz500747t.

(39) Thordarson, P. Determining Association Constants from Titration Experiments in Supramolecular Chemistry. *Chem. Soc. Rev.* **2011**, *40*, 1305–1323. https://doi.org/10.1039/C0CS00062K.

(40) Yang, S. K.; Ambade, A. V.; Weck, M. Supramolecular ABC Triblock Copolymers via One-Pot, Orthogonal Self-Assembly. *J. Am. Chem. Soc.* **2010**, *132*, 1637–1645. https://doi.org/10.1021/ja908429e.

(41) Pahnke, K.; Brandt, J.; Gryn'ova, G.; Lindner, P.; Schweins, R.; Schmidt, F. G.; Lederer, A.; Coote, M. L.; Barner-Kowollik, C. Entropy Driven Chain Effects on Ligation Chemistry. *Chem. Sci.* **2015**, *6*, 1061–1074. https://doi.org/10.1039/C4SC02908A.

(42) Pahnke, K.; Altintas, O.; Schmidt, F. G.; Barner-Kowollik, C. Entropic Effects on the Supramolecular Self-Assembly of Macromolecules. *ACS Macro Lett.* **2015**, *4*, 774–777. https://doi.org/10.1021/acsmacrolett.5b00335.

(43) Elacqua, E.; Lye, D. S.; Weck, M. Engineering Orthogonality in Supramolecular Polymers: From Simple Scaffolds to Complex Materials. *Acc. Chem. Res.* **2014**, *47*, 2405–2416. https://doi.org/10.1021/ar500128w.

(44) Stals, P. J. M.; Gillissen, M. A. J.; Nicolaÿ, R.; Palmans, A. R. A.; Meijer, E. W. The Balance between Intramolecular Hydrogen Bonding, Polymer Solubility and Rigidity in Single-Chain Polymeric Nanoparticles. *Polym. Chem.* **2013**, *4*, 2584-2597. https://doi.org/10.1039/c3py00094j.

(45) Hase, Y.; Nagai, K.; Iida, H.; Maeda, K.; Ochi, N.; Sawabe, K.; Sakajiri, K.; Okoshi, K.; Yashima, E. Mechanism of Helix Induction in Poly(4-Carboxyphenyl Isocyanide) with Chiral Amines and Memory of the Macromolecular Helicity and Its Helical Structures. *J. Am. Chem. Soc.* **2009**, *131*, 10719–10732. https://doi.org/10.1021/ja904128d.

(46) Schwartz, E.; Koepf, M.; Kitto, H. J.; Nolte, R. J. M.; Rowan, A. E. Helical Poly(Isocyanides): Past, Present and Future. *Polym. Chem.* **2011**, *2*, 33–47. https://doi.org/10.1039/C0PY00246A.

(47) Nakahira, T.; Fan, L.; Boon, C. T.; Fukada, T.; Karato, T.; Annaka, M.; Yoshikuni, M. Effects of Side-Chain Structure and Solvent on Intramolecular Hydrogen Bonding in Isotactic Poly(Methacrylamide)s. *Polym. J.* **1998**, *30*, 910–914. https://doi.org/10.1295/polymj.30.910

(48) Zhou, L.; Li, C.-L.; Gao, R.-T.; Kang, S.-M.; Xu, L.; Xu, X.-H.; Liu, N.; Wu, Z.-Q. Highly Regioselective and Helix-Sense Selective Living Polymerization of Phenyl and Alkoxyallene Using Chiral Nickel(II) Catalysts. *Macromolecules* **2021**, *54*, 679–686. https://doi.org/10.1021/acs.macromol.0c02198.

TABLE OF CONTENTS FIGURE

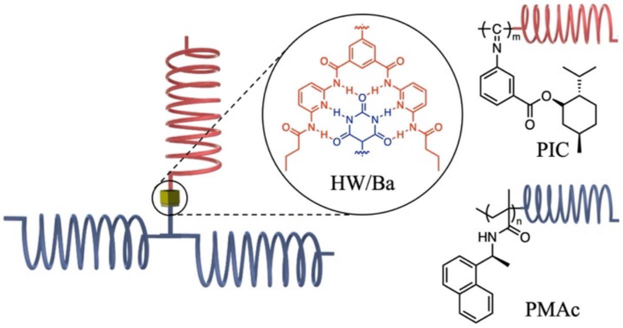

Supramolecular miktoarm star polymers featuring two distinct helical arms connected by hydrogen bonding between Hamilton Wedge and barbituric acid.